

## Vulnerability Level 2 Criterion for Pure-Loss of Stability

Vadim Belenky and Christopher Bassler

*Naval Surface Warfare Center, Carderock Division (David Taylor Model Basin)*

The procedure described for vulnerability level 2 criterion for pure-loss of stability addresses some of the considerations identified in Bassler, et al. (2009) and uses the framework outlined in Belenky, et al. (2009).

### ***Description of the Deterministic Method***

A deterministic method was initially developed as a preliminary demonstration tool; however it can be considered as a deterministic alternative to the probabilistic method described herein.

### **Wave definition**

For the deterministic method, the wave characteristics have to be chosen based on certain considerations.

The wave length is chosen to be equal to ship length, as the change in stability in longitudinal waves is most evident for this condition.

$$\lambda = L \quad (1)$$

Wave height also has been chosen to focus on stability changes. Based on a limited set of calculations, the wave amplitude was set up as:

$$a_w = 0.25d \quad (2)$$

Where  $d$  is draft. The wave elevation along the ship length is defined as:

$$\zeta(t, x, x_c) = a_w \cos(k(x - x_c) - \omega_e t) \quad (3)$$

Here  $k$  is wave number, or spatial frequency. It is related to wave length as:

$$k = \frac{2\pi}{\lambda} \quad (4)$$

$x$  is a coordinate where the wave elevation is being calculated,  $x_c$  location of the wave crest in ship fixed coordinates. The wave frequency of encounter  $\omega_e$  is defined as

$$\omega_e = \omega_w - kV_s \cos(\chi) \quad (6)$$

$V_s$  is speed of the ship while  $\chi$  is the wave direction (0 – following waves).  $\omega_w$  is the wave frequency, determined from the dispersion relation:

$$k = \frac{\omega_w^2}{g} \quad (7)$$

where  $g$  is gravitational acceleration.

## Geometry Definition and a Numerical Example

The geometry of a hull is defined by a number (not less than 20) of stations. To illustrate the method of evaluation, data for ONR Topside Series tumblehome configuration is used (Bishop, et al., 2005). Its geometry is shown in Figure 1, while the main particulars are shown in Table 1. Calculation of other sample ships is discussed separately below.

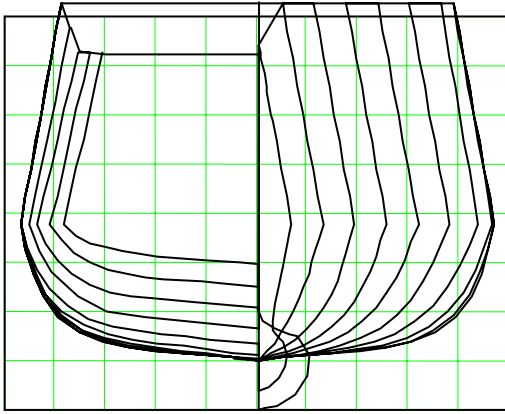


Figure 1. Geometry of the ONR tumblehome topside configuration

Table 1. Principal Particulars

|                |      |
|----------------|------|
| Length, BP, m  | 154  |
| Breadth, B, m  | 18.8 |
| Depth, D, m    | 12.5 |
| Draft, m       | 5.5  |
| Critical GM, m | 2.01 |

## Evaluation of GM in Waves

The area at each station and its moment relative to the vertical axis are expressed as function of the local draft, accounting for the sinkage and the trim:

$$A_i(z) = 2 \int_0^z b_i(z) dz \quad M_{z_i}(z) = 2 \int_0^z z b_i(z) dz \quad (8)$$

$i$  indicates the station number,  $b_i(z)$  is the half-breadth at station  $i$ , at the local draft  $z$ . The volumetric displacement can be expressed as a function of the position of a wave crest an array of local drafts  $\vec{z} = \{z_i\}, i = 1, N_s$ :

$$V(x_C, \vec{z}) = 0.5 \sum_{i=1}^{N_s-1} (A_i(z_i) + A_{i+1}(z_{i+1})) (x_{i+1} - x_i) \quad (9)$$

$x_i$  is the coordinate of the  $i$ -th station in the ship-fixed coordinate system.

The moments of the hull relative to vertical and longitudinal axes are expressed using a similar formulation:

$$MZ(x_C, \bar{z}) = 0.5 \sum_{i=1}^{N_{st}-1} (Mz_i(z_i) + Mz_{i+1}(z_{i+1}))(x_{i+1} - x_i) \quad (10)$$

$$MX(x_C, \bar{z}) = 0.5 \sum_{i=1}^{N_{st}-1} (x_i A_i(z_i) + x_{i+1} A_{i+1}(z_{i+1}))(x_{i+1} - x_i) \quad (11)$$

Formulae (9) and (11) can be used to express coordinates for the center of buoyancy:

$$LCB(x_C, \bar{z}) = \frac{MX(x_C, \bar{z})}{V(x_C, \bar{z})}; \quad KB(x_C, \theta, z_S) = \frac{MZ(x_C, \bar{z})}{V(x_C, \bar{z})} \quad (12)$$

The local draft at each station comes from formula (3), describing wave elevations along the hull, and depends on sinkage and trim. Consideration of time for the change of stability in waves is redundant and the wave profile along the hull is considered as a function of wave crest position only.

$$\zeta(x, x_C) = a_w \cos(k(x - x_C)) \quad (13)$$

To account for the trim on the wave profile, the following auxiliary function is introduced:

$$\Xi(x_i, z_i, \theta, x_C) = a_w \cos[k(x_i \cos \theta - z_i \sin \theta - x_C)] - (x_i \sin \theta + z_i \cos \theta) \quad (14)$$

This function equals zero when a point with coordinates  $x_i$  and  $z_i$  is exactly at the surface of the wave of amplitude  $a_w$ , rotated by the trim angle  $\theta$ . Then the elevation of the wave profile at the  $i$ -th station is defined through the inverse of the function  $\Xi$ , calculated for each station located at  $x_i$ :

$$z_{wL}(\theta, z_S, x_i, x_C) = INV(\Xi(x_i, z_i, \theta, x_C)) + z_S \quad (15)$$

where  $z_S$  is the sinkage.

The wave profile along the ship hull is evaluated by satisfying equilibrium conditions through solving the following system of nonlinear algebraic equations, with trim and sinkage as unknowns

$$\begin{cases} V(x_C, z_{wL}(\theta, z_S, x_i, x_C)) = V_0 \\ LCB(x_C, z_{wL}(\theta, z_S, x_i, x_C)) = LCB_0 \end{cases} \quad (16)$$

Once sinkage and trim are found, the profile of the wave along the hull can be found as:

$$z_i = z_{wL}(\theta, z_S, x_i, x_C) \quad (17)$$

The moment of inertia of the waterplane made by the wave profile is:

$$I_X(x_C) = \frac{1}{3} \sum_{i=1}^{N_{st}-1} (b^3(z_i) + b^3(z_{i+1})) (x_{i+1} - x_i) \quad (18)$$

Other hydrostatic terms are also needed to determine GM

$$KB(x_C) = \frac{MZ(x_C, \bar{z})}{V_0}; \quad BM(x_C) = \frac{I_X(x_C)}{V_0} \quad (19)$$

Finally the value of GM in waves is a function of the position of a wave crest

$$GM(x_C) = BM(x_C) - KG + KB(x_C).$$

### Importance of Balancing for GM in Waves

It is known that balancing a ship with sinkage and trim may significantly change the result for determining GZ in waves. To demonstrate this effect, the calculations described above can be complemented by partial balancing (sinkage/displacement only) or no balancing results. This demonstration is important, because balancing is the most intensive part of the calculation.

Partial balancing is implemented by setting  $\theta = \theta_0$  (to calm water value) in formula (15); this converts a system of equations into a single equation:

$$V(x_C, z_{WL}(\theta = \theta_0, z_S, x_i, x_C)) = V_0 \quad (20)$$

Results for the moment of inertia of the area of the waterplane are shown in Figure 2:

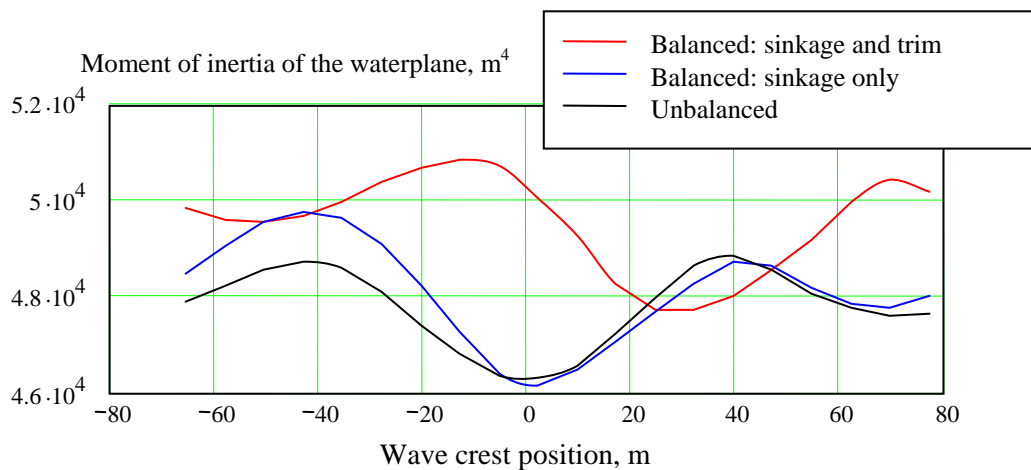


Figure 2. Change of the moment of inertia of the area of the waterline with moving wave crest for different type of balancing for ONR tumblehome topside ship

It is clear from Figure 2 that balancing both sinkage and trim results in a significant difference for the moment of inertia of the waterplane. It can also be seen from Figure 3, which shows the change of  $BM$ . The calculation of  $BM$  without balancing is done using the resulting volumetric displacement from that wave crest position:

$$BM(x_c) = \frac{I_x(x_c)}{V(x_c, \bar{z})} \quad (21)$$

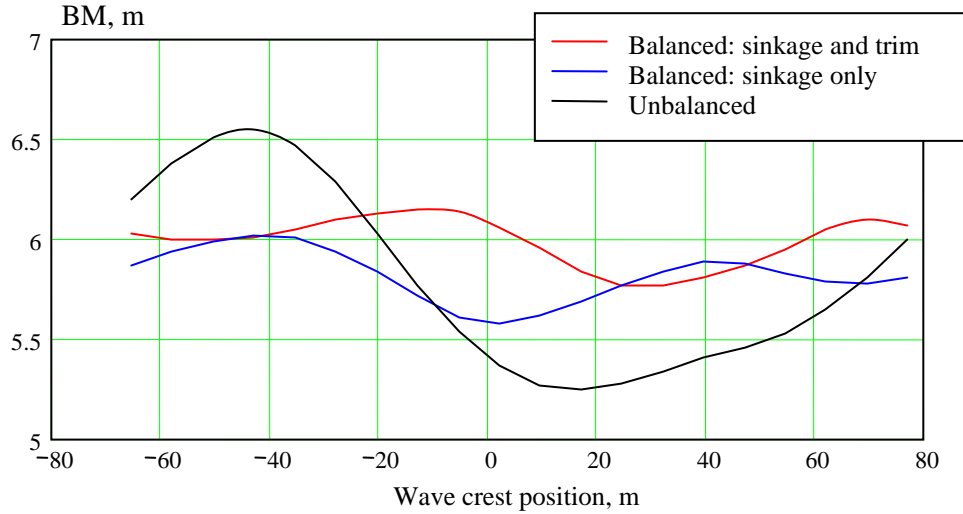


Figure 3. Change of the  $BM$ -value with moving wave crest for different type of balancing for ONR tumblehome topside ship

A similar approach was used to calculate the unbalanced  $KB$ , which is shown in Figure 4.

$$KB(x_c) = \frac{MZ(x_c, \bar{z})}{V(x_c, \bar{z})} \quad (22)$$

As seen in Figure 4, balancing with sinkage has the most influence for the  $KB$  value. Figure 5 shows  $GM$  in waves calculated with different balancing options. It is clear from Figure 5 that these balancing options have a significant influence on the initial stability in waves. Two features should also be noted. First, the magnitude of the change of stability is the largest for the unbalanced results. Second, the ONR tumblehome topside ship is an example of an unconventional vessel and therefore, these conclusions are not general.

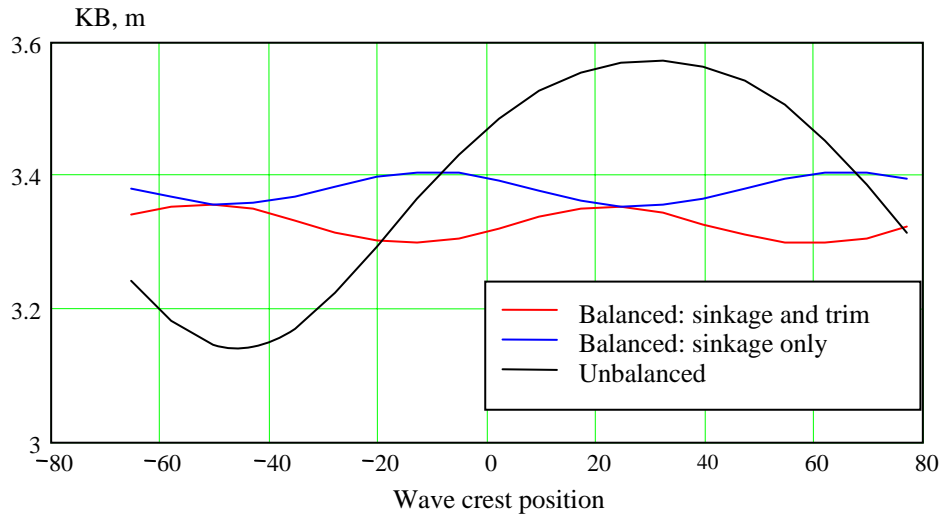


Figure 4. Change of the  $KB$ -value with moving wave crest for different type of balancing for ONR tumblehome topside ship

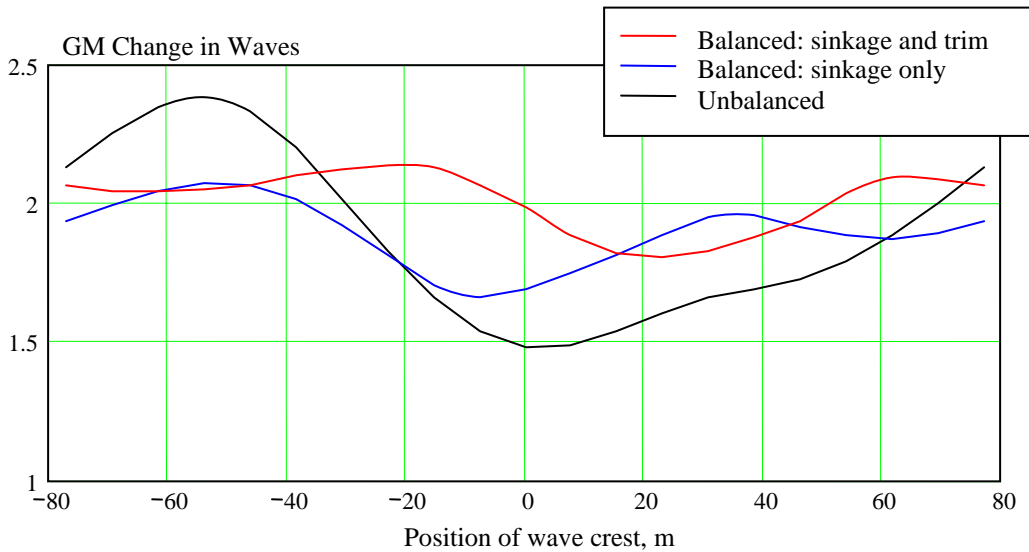


Figure 5. Change of GM in waves with moving wave crest for different type of balancing for ONR tumblehome topside ship

### Approximation of Stability in Waves Using Only GM

Stability change in waves is not limited by GM, the entire GZ curve experiences changes. The main advantage of using GM is simplicity and to enable the possibility to perform spreadsheet style calculations. Using GM only for the evaluation of stability in waves also can be considered as an approximation, where the change of GM in waves is used to “modulate” the calm-water GZ curve.

$$GZ(\phi, x_c) = GZ_0(\phi) - (GM_0 - GM(x_c)) \sin(\phi) \quad (23)$$

To evaluate the level of approximation introduced by “modulation” (23), the entire GZ curve was computed using a preprocessor, PRELMP, of the advanced panel code LAMP (Lin and Yue, 1990; 1993). The preprocessor uses a quasi-static wave and computes the righting moment by integrating pressures around the hull. Another tool capable of performing these calculations is EUREKA (Paulling, 1961). It was demonstrated that PRELMP calculations are identical to EUREKA (Belenky and Weems, 2008). The results of the direct calculation of the GZ curve in waves for the same conditions are shown in Figure 6, while Figure 7 shows the approximate “modulated” GZ curve.

The comparison between GZ curves in Figures 6 and 7 shows the generally conservative character of approximation (23) as the influence of the wave, in general, is slightly exaggerated by the approximation (23). Despite the approximation, which is not capable of presenting all the details of stability change in waves, it still seems to be a reasonable tool for vulnerability-level assessment.

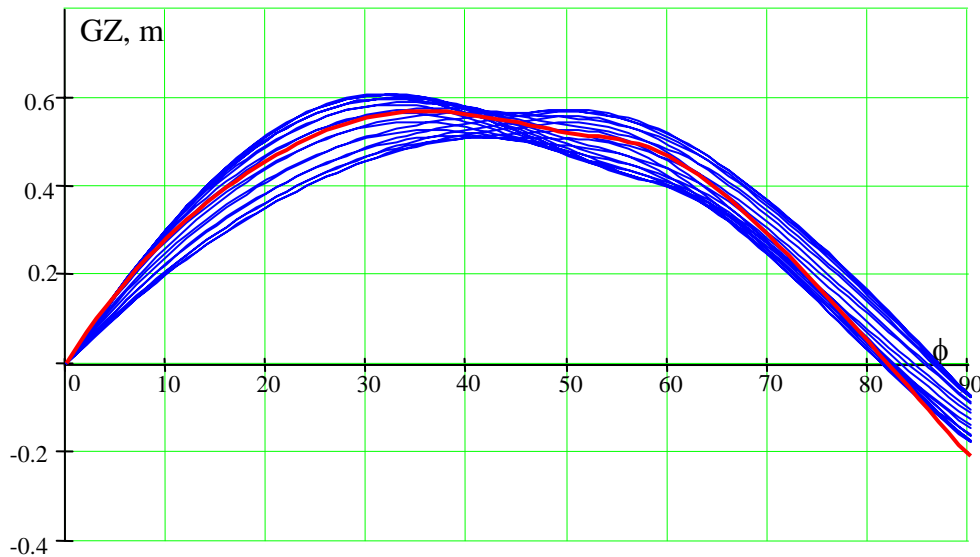


Figure 6. GZ curve of the ONR tumblehome topside ship in wave calculated with PRELMP

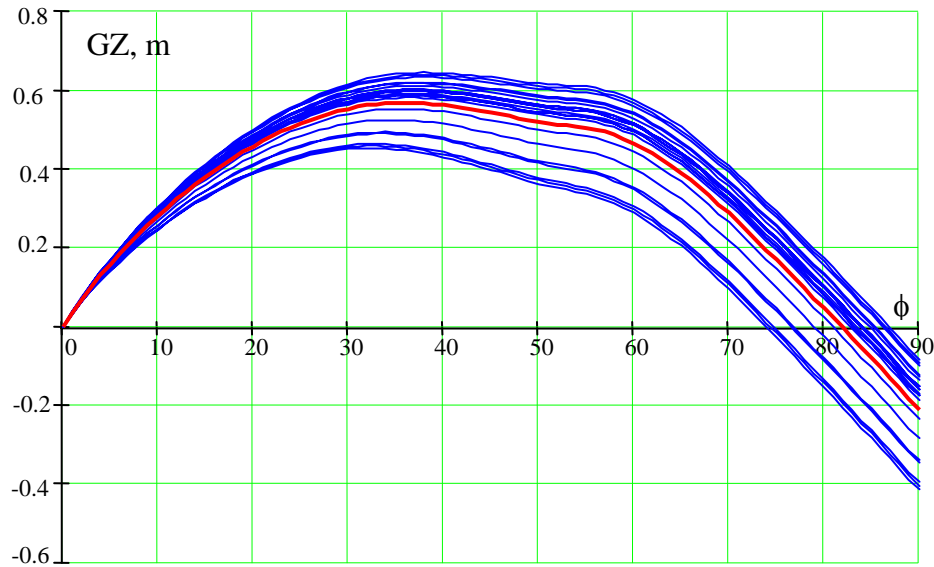


Figure 7. GZ curve in wave of the ONR tumblehome topside ship approximated with formula (23)

## Deterministic Vulnerability Criterion

Stability failure associated with pure-loss of stability occurs when stability is decreased while the ship is located on the wave crest. If a heeling moment is applied while the stability is decreased, the ship may develop a significant roll angle, or even capsize, therefore, vulnerability to pure-loss of stability is effectively related to the time duration where the stability is reduced.

Another factor for consideration is loading condition, KG in particular. If the KG value is small enough, the decrease of stability while the ship is located on the wave crest would not create much of a problem, because a sufficient reserve of stability remains to counter the heeling moment. Therefore, the position of KG must be determined for vulnerability assessment.

The idea of vulnerability assessment is focused on distinguishing between conventional and unconventional vessels. Unconventional vessels may experience a stability failure on the wave crest, due to their unusual hull geometry, where a conventional ship is not subjected to additional risk.

Nevertheless, a conventional ship also experiences a decrease of stability in the wave crest. However this risk was implicitly accounted for, as the existing criteria are based on the experience of operation and expressed through statistics of stability failures.

Consider a conventional vessel, with KG corresponding to a critical condition. If a wave passes such a ship from the stern, it will spend some time near the wave crest and her stability will decrease below the critical level. As this situation is implicitly included in the current regulation,

the time the conventional ship spends at the wave crest can be considered acceptable, while significant exceedance of this time may be used as an indication of vulnerability. Summarizing the considerations above, vulnerability assessment considers

- Loading conditions, corresponding to critical KG
- Following waves direction with an assumed speed
- Time duration when the GM-value below critical is calculated
- The “time-below-critical-GM” is expected to be longer for unconventional vessels than for conventional vessels.

To calculate the time-below-critical-GM, the intersections should be between the GM in waves and the line corresponding to critical GM, see Figure 8.

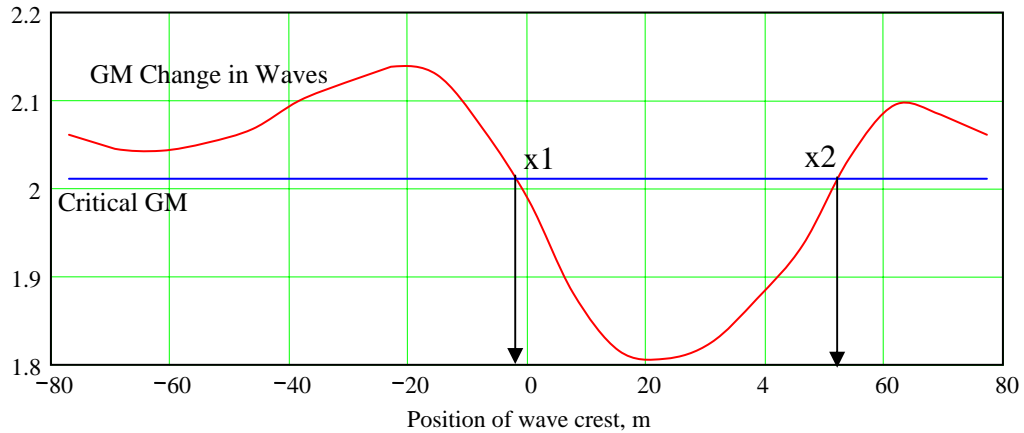


Figure 8. Calculation of “time-below-critical-GM”

Points x1 and x2 in Figure 8 show the distance when the GM remains below the critical level, while the wave passes the ship. The time duration can be calculated as:

$$tbc = \frac{x2 - x1}{c - V_s} \quad (24)$$

where  $c$  is wave celerity and  $V_s$  is ship speed.

Assuming the ship speed to be 5 knots for the ONR tumblehome topside ship, the time-below-critical-GM was found to be 4.2 seconds. The natural period of roll was estimated about 10.6 s, so the time-below-critical-GM represented about 40% of the duration of the natural roll period.

## Standard for Deterministic Vulnerability Criterion

While the ONR tumblehome topside ship can be considered as a good candidate for an unconventional vessel, the flared hull from the ONR topside series (Bishop, et al., 2005) represents a more conventional ship, not known for experiencing stability failures related to pure-loss of stability. The lines for this ship are shown in Figure 9 and principal particulars in Table 2. An example of an even more conventional ship is Series 60 (Todd, 1953). Its lines are shown in Figure 10 and principal particulars in Table 3

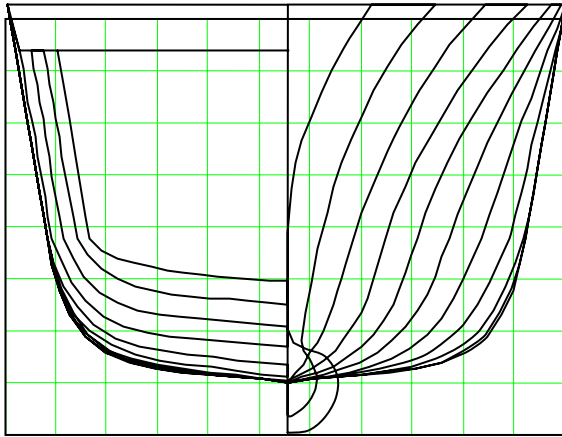


Figure 9. Geometry of the ONR flared topside configuration

Table 2. Principal Particulars ONR flared

|                |      |
|----------------|------|
| Length, BP, m  | 154  |
| Breadth, B, m  | 18.8 |
| Depth, D, m    | 12.5 |
| Draft, m       | 5.5  |
| Critical GM, m | 0.19 |

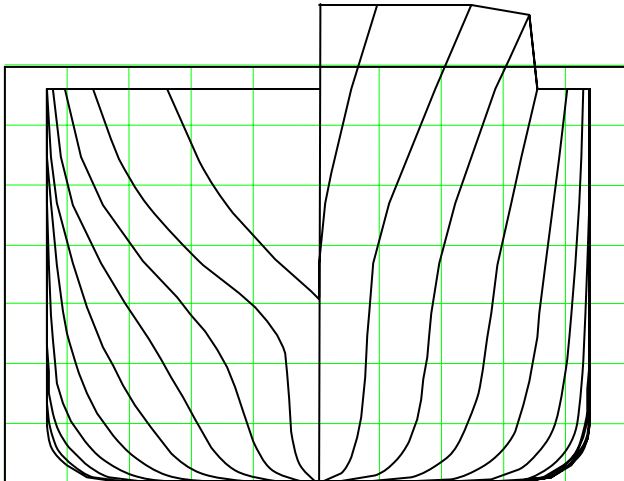


Figure 10. Geometry of the Series 60  $C_B=0.7$

Table 3. Principal Particulars – Series 60

|                |        |
|----------------|--------|
| Length, BP, m  | 121.92 |
| Breadth, B, m  | 17.4   |
| Depth, D, m    | 13.15  |
| Draft, m       | 6.97   |
| Critical GM, m | 0.15   |

The same sequence of calculations described in the previous section was applied to these ships. Figure 11 shows the change in GM, while the wave passes with critical GM for the ONR topside series flared configuration. The critical GM was evaluated using Sarchin & Goldberg criteria (Sarchin and Goldberg, 1962). Figure 12 shows similar results for the Series 60 hull. The critical GM value for the Series 60 was evaluated using the current IMO criteria.

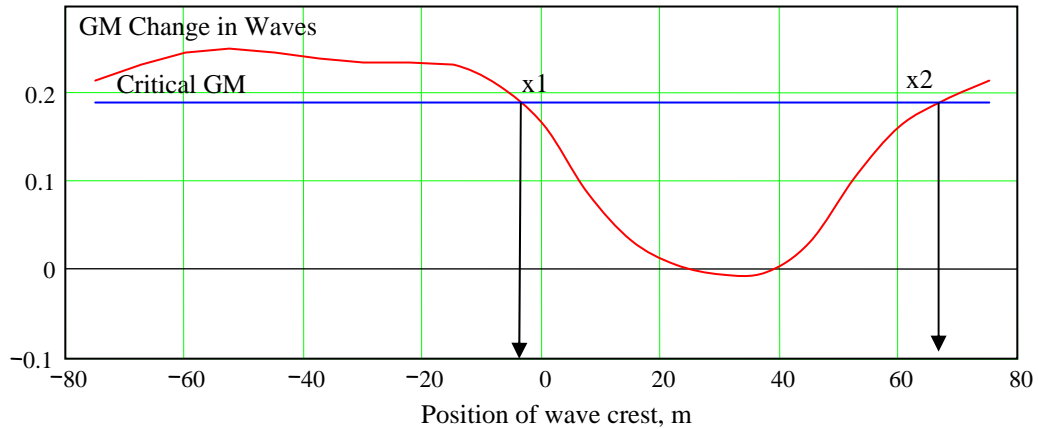


Figure 11. Calculation of “time-below-critical-GM” for ONR flared hull

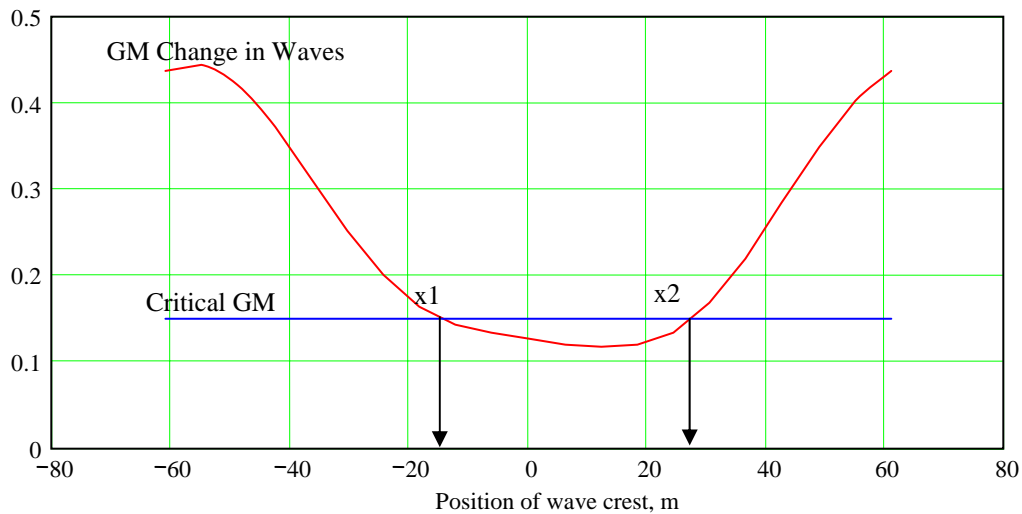


Figure 12. Calculation of “time-below-critical-GM” for Series 60,  $C_B=0.7$

The results for the C11-class containership data are shown in Figure 14 (see lines in Figure 13, principal particulars in Table 4). This ship is known to be vulnerable to parametric roll and therefore, may experience significant changes of the GZ curve in waves. The results of calculations comparing all four ships are shown in Table 5 and Figure 15 for comparison.

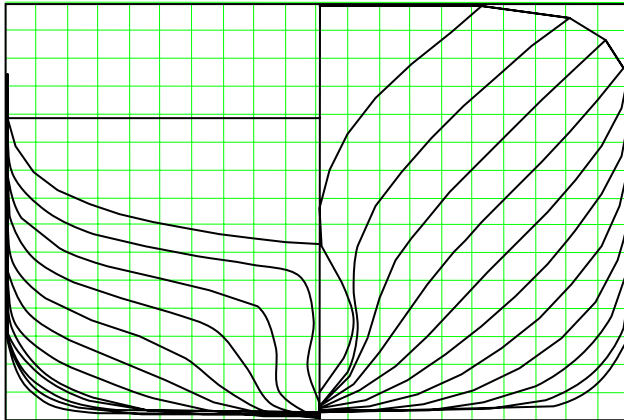


Figure 13. Geometry of the C11-class containership

Table 4. Principal Particulars – C11

|                |       |
|----------------|-------|
| Length, BP, m  | 262   |
| Breadth, B, m  | 49    |
| Depth, D, m    | 24.7  |
| Draft, d, m    | 12.83 |
| Critical GM, m | 1.63  |

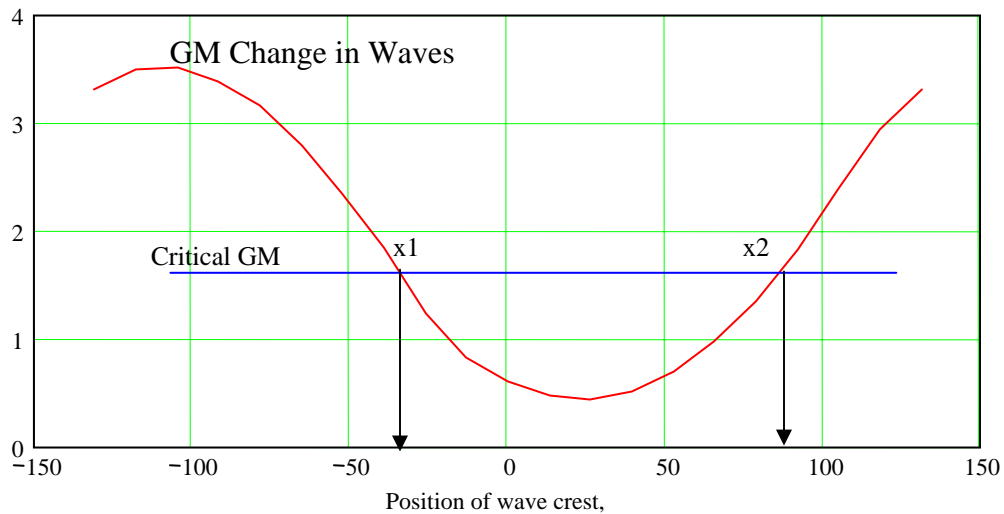


Figure 14. Calculation of “time-below-critical-GM” for C11-class containership

All the calculations were repeated for several speeds, at 5, 10, and 15 knots. As expected, the value of the “time-below-critical-GM” is sensitive to speed. As the speed increases, a ship spends more time near the wave crest. However, this dependence seems to be monotonic, so only one speed can be used for setting the vulnerability boundary.

Table 5. Summary Table for the Time-below-critical-GM

|   | Series 60,<br>$C_B=0.7$ | ONR Flared | C11   | ONR<br>Tumblehome |
|---|-------------------------|------------|-------|-------------------|
| Critical GM, m  | 0.15                    | 0.19       | 1.63  | 2.01              |
| Distance traveled below<br>critical GM, as a fraction<br>of ship length | 0.352                   | 0.469      | 0.464 | 0.352             |
| Natural roll period, s  | 35.9                    | 34.5       | 25    | 10.6              |
| Speed, kn   | 5                       | 5          | 5     | 5                 |
| Time-below-critical-GM, s   | 2.3                     | 5.5        | 6.88  | 4.2               |
| Fraction of the natural roll<br>period                                  | 0.11                    | 0.16       | 0.28  | 0.4               |
| Speed, kn   | 10                      | 10         | 10    | 10                |
| Time-below-critical-GM, s   | 4.96                    | 6.92       | 8.06  | 5.23              |
| Fraction of the natural roll<br>period                                  | 0.138                   | 0.2        | 0.32  | 0.5               |
| Speed, kn   | 15                      | 15         | 15    | 15                |
| Time-below-critical-GM, s   | 7.06                    | 9.27       | 9.71  | 10.6              |
| Fraction of the natural roll<br>period                                  | 0.2                     | 0.27       | 0.39  | 0.656             |

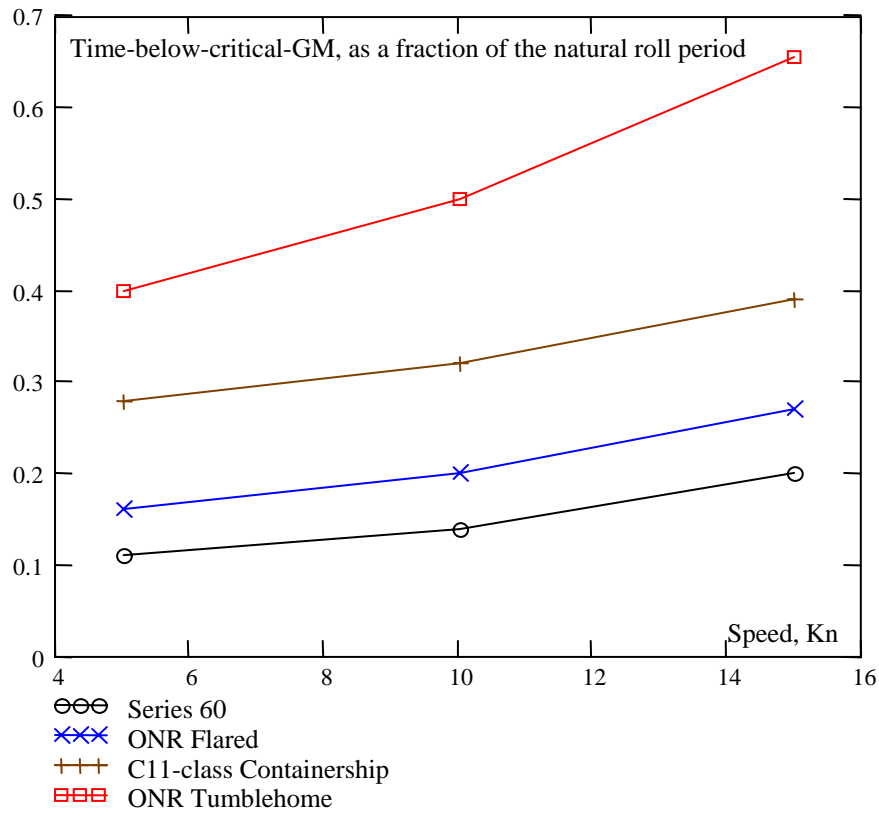


Figure 15. Dependence of the time-below-critical-GM, expressed as a fraction of the natural roll period

Figure 15 illustrates differences between conventional ships, which are not vulnerable to pure-loss of stability, and an unconventional ship, which is vulnerable, in this case as a function of ship speed.

### **Description of the Probabilistic Method**

The probabilistic version of the present method does not necessitate arbitrary assumptions on wave characteristics. It considers a ship sailing with forward speed in irregular long-crested waves, defined with a given spectrum.

### **Wave Model**

To avoid the application of Monte-Carlo methods with associated uncertainties, the envelope method is used to present the stochastic process of wave elevations:

$$\zeta(t, x) = A(t, x) \cos(\Psi(x) - \Phi(t)) \quad (25)$$

where  $A(t)$  is a stochastic process of the envelope, which can also be considered as amplitudes,  $\Psi(x)$  is a stochastic process of phases in space, and  $\Phi(t)$  is a stochastic process of phases in time.

Changes of stability are immediate, therefore, consideration of time is not required and the wave elevation can be considered only as a spatial stochastic process:

$$\zeta(x) = A(x) \cos(\Psi(x)) \quad (26)$$

The wave elevations are known to have a normal distribution, and envelope follows a Rayleigh distribution:

$$f(A) = \frac{A}{V_\zeta} \exp\left(-\frac{A^2}{2V_\zeta}\right) \quad (27)$$

where  $V_\zeta$  is variance of wave elevations.

The distribution of the spatial phase is uniform:

$$f(\Psi) = \begin{cases} \frac{1}{2\pi} & 0 < \Psi \leq 2\pi \\ 0 & \textit{otherwise} \end{cases} \quad (28)$$

Envelope theory also allows the distribution to be expressed as the derivative of the phase:

$$\dot{\Psi} = \frac{d\Psi}{dx} \quad (29)$$

$$f(\dot{\Psi}) = \frac{k_2^2 - k_1^2}{2\left(\sqrt{(\dot{\Psi} - k_1)^2 + (k_2^2 - k_1^2)}\right)^3}$$

where  $k_1$  is the mean wave number.

$$k_1 = \frac{1}{V_\zeta} \int_0^\infty \frac{\omega^2}{g} s(\omega) d\omega \quad (30)$$

The value of  $k_2$  can be interpreted as a mean spectrum band in terms of wave number.

$$k_2 = \sqrt{\frac{1}{V_\zeta} \int_0^\infty \frac{\omega^4}{g^2} s(\omega) d\omega} \quad (31)$$

The amplitudes and phases are independent, however amplitudes and derivatives of phases are dependent and their joint distribution can also be determined from envelope theory:

$$f(A, \dot{\Psi}) = \frac{A^2}{\sigma_\zeta^3 \sqrt{k_2^2 - k_1^2} \sqrt{2\pi}} \exp\left(-A^2 \frac{k_2^2 - 2k_1 \dot{\Psi} + \dot{\Psi}^2}{2\sigma_\zeta^2 (k_2^2 - k_1^2)}\right) \quad (32)$$

The shape of the distribution (32) calculated for sea state 8 (Bretshneider spectrum with significant wave height 11.5 m and modal period 16.4 s) is shown in Figure 16.

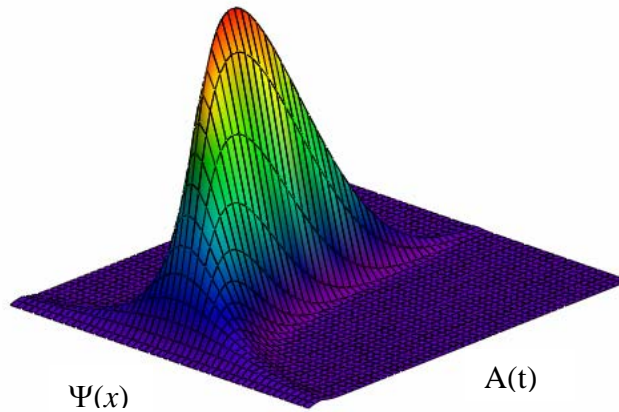


Figure 16. Joint distribution of amplitudes and derivatives of phases for the envelope presentation

The derivative of the phase is usually associated with a random wave number, which is also considered as a stochastic process. Such consideration corresponds to the following first-order approximation:

$$\zeta(x) = A(x)\cos(\dot{\Psi}(x)x) \quad (33)$$

where  $\dot{\Psi}(x)$  plays a role of random wave number.

As a result, the irregular seaway can be presented as a set of harmonic waves of random length and amplitudes. The probability of encounter of a wave with a certain height (amplitude) and length (wave number) can be calculated from the distribution (32).

Because stability change in waves is limited to waves comparable with ship length, it makes sense to limit consideration of the wave characteristics to the wave number corresponding to wave lengths from 0.5L to 1.5L. Wave amplitude was limited by 80% of the draft to avoid problems with non-convergence during balancing. This may appear to be a limitation for smaller vessels. *However, waves of large height are more likely to have larger length and waves of large length (in comparison with ship length) are not going to greatly affect stability.*

Statistical weight of a wave with an amplitude  $A_i$  and wave number  $k_j$  is calculated as:

$$W_{ij} = \int_{A_i-\Delta A}^{A_i+\Delta A} \int_{k_j-\Delta k}^{k_j+\Delta k} f(A, k) dk dA \quad (34)$$

Once a wave and its statistical weight have been defined, further stability calculations may be carried out.

## Evaluation of Stability Changes in Irregular Waves

Because irregular waves are presented in the form of a single harmonic, the algorithm described previously for regular waves is used. The only difference is the number of parameters considered. For regular waves, it was only one, varying the position of the wave crest. For irregular waves, there are three, including amplitude, wave number and the position of the wave crest.

In an attempt to limit calculation time, only two wave crest positions are used: wave crest and wave trough near amidships. However, this simplification may decrease the sensitivity of the criterion, as the most significant stability decrease for all ships is not necessarily when the wave crest is exactly amidships. This situation can be seen in Figure 8, where the worst decrease of stability has occurred, when the wave crest was about 20 m forward of the mid-ship section. Applicability of this simplification can be checked by changing the position of wave crest to observe if there is a significant difference in the value of the criterion.

As a result of this simplification, two  $GM$  values are produced for each wave:  $GM_{c_{ij}}$  – for the wave crest amidships and  $GM_{t_{ij}}$  – for the wave trough amidships. This allows amplitude and mean  $GM$  change to be introduced for each wave:

$$GMa_{ij} = 0.5(GMt_{ij} - GMc_{ij}) \quad (35)$$

$$GMm_{ij} = 0.5(GMt_{ij} + GMc_{ij}) \quad (36)$$

The approximation for stability change is expressed as:

$$GM(x, i, j) = GMm_{ij} - GMa_{ij} \cos(k_{ij}x) \quad (37)$$

The time-below-the-critical-GM the can be expressed as:

$$tbc_{ij} = \frac{1}{c_{ij} - V_s} \frac{2}{k_{ij}} \arccos\left(\frac{GMm_{ij} - GM_{crit}}{GMa_{ij}}\right) \quad (38)$$

Formula (38) is a deterministic function of random variables. In general terms it can be expressed as:

$$tbc = \varphi(A, k) \quad (39)$$

A mean value of the deterministic function of two random variables is formally expressed as:

$$m(tbc) = \int_0^{\infty} \int_{-\infty}^{\infty} \varphi(A, k) f(A, k) dk dA \quad (40)$$

Note that because the wave number has been defined using the derivative of the spatial phase it can take negative values. To calculate the mean value of time-below-critical-GM, statistical weights (34) are to be used:

$$m(tbc) = \sum_i \sum_j tbc_{ij} W_{ij} \quad (41)$$

The ratio of  $m(tbc)$  over the natural roll period represents a probabilistic version of the level 2 vulnerability criterion for pure-loss of stability.

## Sample Calculations for Probabilistic Criteria

Sample calculations were performed for the same ships described previously. These calculations were completed for 5, 10, and 15 knots, and include sea states 5, 6, 7 and 8. The results are detailed in Table 6. The trend for speed dependence for a constant sea state is shown in Figure 17. The trend for changing sea state with fixed speed is shown in Figure 18.

Comparing the sample calculation for the deterministic criterion in Figure 15 to the probabilistic criterion in Figures 17 and 18, it can be observed that the probabilistic criterion provides greater distinction between the ONR tumblehome topside hull, which is known to be vulnerable to pure-loss of stability (Bishop, et al., 2005; Bassler, et al., 2007; Hashimoto, 2009), compared to other ships, which are not known to be vulnerable to this type of stability failure.

Table 6. Summary table for mean time-below-critical-GM

|   | Series 60 | ONR Flared | C11   | ONR<br>Tumblehome |
|---|-----------|------------|-------|-------------------|
| Critical GM, m  | 0.15      | 0.19       | 1.63  | 2.01              |
| Distance traveled below critical GM, as a fraction of ship length | 0.352     | 0.469      | 0.464 | 0.352             |
| Natural roll period, s  | 35.9      | 34.5       | 25    | 10.6              |
| Sea state   | 8         | 8          | 8     | 8                 |
| Speed, kn   | 5         | 5          | 5     | 5                 |
| Time-below-critical-GM, s   | 1.7       | 6.784      | 4.66  | 8.824             |
| Fraction of natural roll period                                   | 0.048     | 0.197      | 0.186 | 0.754             |
| Speed, kn   | 10        | 10         | 10    | 10                |
| Time-below-critical-GM, s   | 2.07      | 7.98       | 5.362 | 10.7              |
| Fraction of natural roll period                                   | 0.057     | 0.23       | 0.214 | 0.913             |
| Speed, kn   | 15        | 15         | 15    | 15                |
| Time-below-critical-GM,s  | 2.54      | 9.74       | 6.35  | 13.73             |
| Fraction of natural roll period                                   | 0.071     | 0.28       | 0.254 | 1.17              |
| Sea state   | 7         | 7          | 7     | 7                 |
| Speed, kn   | 5         | 5          | 5     | 5                 |
| Time-below-critical-GM, s   | 2.136     | 6.788      | 4.095 | 7.1               |
| Fraction of natural roll period                                   | 0.06      | 0.197      | 0.163 | 0.61              |
| Speed, kn   | 10        | 10         | 10    | 10                |
| Time-below-critical-GM, s   | 2.58      | 8.06       | 4.725 | 8.79              |
| Fraction of natural roll period                                   | 0.072     | 0.234      | 0.189 | 0.751             |
| Speed, kn   | 15        | 15         | 15    | 15                |
| Time-below-critical-GM, s   | 3.28      | 10.0       | 5.62  | 11.67             |
| Fraction of natural roll period                                   | 0.091     | 0.29       | 0.224 | 0.997             |
| Sea state   | 6         | 6          | 6     | 6                 |
| Speed, kn   | 5         | 5          | 5     | 5                 |
| Time-below-critical-GM, s   | 2.015     | 5.717      | 2.78  | 5.125             |
| Fraction of natural roll period                                   | 0.056     | 0.166      | 0.111 | 0.438             |
| Speed, kn   | 10        | 10         | 10    | 10                |
| Time-below-critical-GM, s   | 2.487     | 6.94       | 3.25  | 6.6               |
| Fraction of natural roll period                                   | 0.069     | 0.2        | 0.128 | 0.563             |
| Speed, kn   | 15        | 15         | 15    | 15                |
| Time-below-critical-GM, s   | 3.307     | 8.99       | 3.81  | 9.364             |
| Fraction of natural roll period                                   | 0.092     | 0.261      | 0.152 | 0.8               |

Table 6. Summary table for mean time-below-critical-GM (Cont.)

|   | Series 60 | ONR Flared | C11   | ONR Tumblehome |
|---|-----------|------------|-------|----------------|
| Critical GM, m  | 0.15      | 0.19       | 1.63  | 2.01           |
| Distance traveled below critical GM, as a fraction of ship length | 0.352     | 0.469      | 0.464 | 0.352          |
| Natural roll period, s  | 35.9      | 34.5       | 25    | 10.6           |
| Sea state   | 5         | 5          | 5     | 5              |
| Speed, kn   | 5         | 5          | 5     | 5              |
| Time-below-critical-GM, s   | 1.665     | 3.621      | 1.569 | 2.92           |
| Fraction of natural roll period                                   | 0.046     | 0.105      | 0.063 | 0.249          |
| Speed, kn   | 10        | 10         | 10    | 10             |
| Time-below-critical-GM, s   | 2.125     | 4.454      | 1.796 | 3.866          |
| Fraction of natural roll period                                   | 0.059     | 0.129      | 0.072 | 0.332          |
| Speed, kn   | 15        | 15         | 15    | 15             |
| Time-below-critical-GM, s   | 3.024     | 5.93       | 2.111 | 5.866          |
| Fraction of natural roll period                                   | 0.084     | 0.172      | 0.084 | 0.501          |

The probabilistic criterion rated the C11-containership class lower than the ONR flared topside hull, while the deterministic criterion rated the flared topside hull lower than C11. This can be explained by difference in the size of these ships. Significant change of stability on a wave crest can be invoked by a wave comparable to the ship length. Naturally occurring longer waves, which can pose a danger to the post-Panamax containership, are rarer than relatively shorter waves which can pose a danger for the ONR flared topside hull. The deterministic criterion used a wave equal to ship length and, therefore, is unable to account for change in size. The probabilistic criterion uses a more realistic wave model, derived from a spectrum and therefore, accounts for the fact that very long waves are rarer.

The value of the criterion for C11 increases faster with increasing sea state (see Figure 18). This can be explained because an increasing sea state leads to increased probability of longer waves, which may affect stability of a post-Panamax containership. This observation is consistent with the previous consideration.

Both the probabilistic and deterministic criteria show similar value for ONR flared hull and C11-class containership. Most likely, this similarity is not random, as both ships have buttock-flow type sterns. The stern shape is known to affect stability change in waves (Levadou and Veer, 2006).

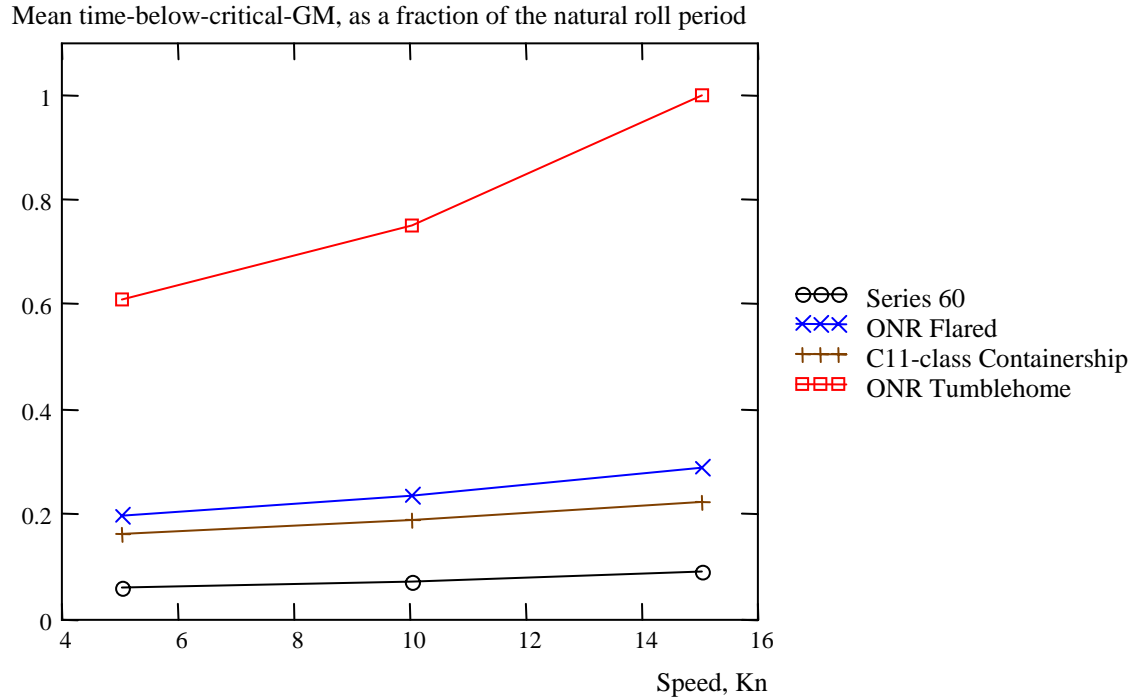


Figure 17. Dependence of the mean time-below-critical-GM, expressed as a fraction of the natural roll period, on forward speed for sea state 7

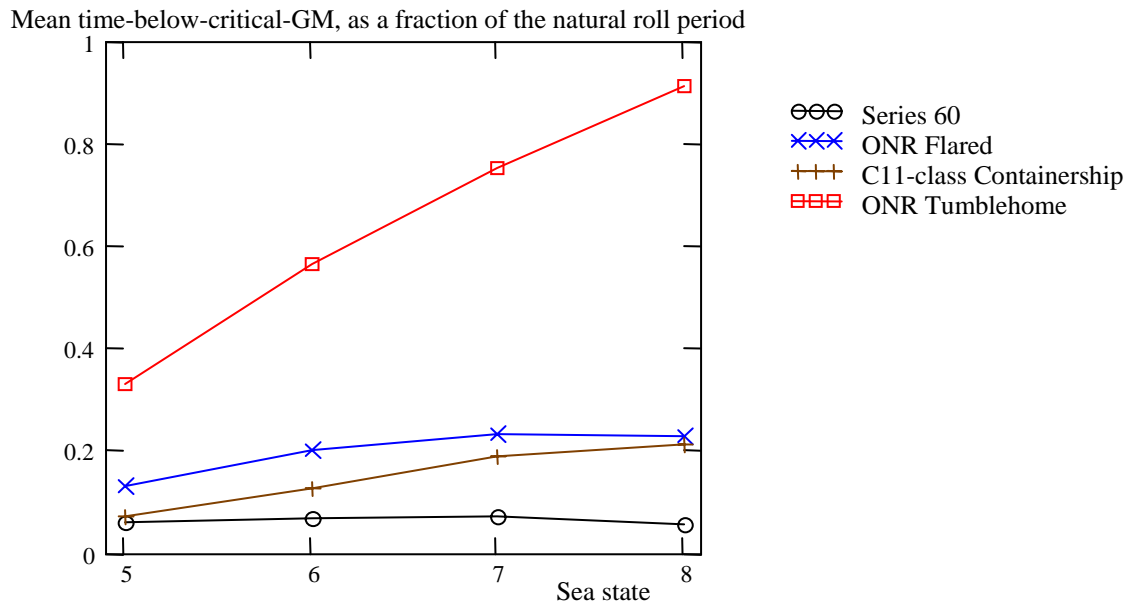


Figure 18. Dependence of the mean time-below-critical-GM, expressed as a fraction of natural roll period, on sea state for forward speed of 10 knots

## **Summary**

A criterion to assess vulnerability to the pure-loss of stability intact stability failure mode was discussed. Both deterministic and probabilistic evaluation methods were presented and used to assess vulnerability for four ships, ranging from very conventional (Series 60) to very unconventional (ONR tumblehome topside). In both formulations, the duration of time spent below critical GM was determined and compared to the natural roll period to provide a baseline metric.

For the deterministic method, the assumption of wave length equal to ship length and wave height equal to 50% of ship draft was used to provide wave characteristics to evaluate vulnerability for pure-loss of stability. Three forward speeds (5, 10, and 15 knots) were assessed. The criterion showed a distinct difference between three conventional ships, with vulnerability increased with additional modern hull form characteristics, and an unconventional hull. All hull forms showed increased vulnerability with increased ship speed. The deterministic criterion may be modified to include consideration for the change in ship size, relative to wave size. However, providing this association will still require some information about the wave conditions. Therefore, a probabilistic method is preferred.

For the probabilistic method, four sea state conditions (sea states 5, 6, 7 and 8, using a Bretschneider spectral formulation) and three forward speeds (5, 10, and 15 knots), the criterion showed distinct differences between the conventional and unconventional vessels. The probabilistic criterion was also able to better distinguish between vulnerability for the ONR flared topside and the C11-class containership, because of consideration of the probability of the occurrence of the wave conditions necessary to increase vulnerability. Generally, the hull forms showed an increase in vulnerability with increased ship speed and an increased sea state.

## **References**

Bassler, C. B., Campbell, W., Belknap, and L. McCue, 2007, "Dynamic Stability of Flared and Tumblehome Hull Forms in Waves," Proc. 9th Intl. Ship Stability Workshop, Hamburg, Germany.

Bassler, C. C., V. Belenky, G. Bulian, A. Francescutto, K. Spyrou, and N. Umeda, 2009, "A Review of Available Methods for Application to Second Level Vulnerability Criteria" Proc. 10th Intl. Conf. on Stability of Ships and Ocean Vehicles, St. Petersburg, Russia.

Belenky, V. and K. M. Weems, 2008, "Probabilistic Qualities of Stability Change in Waves," Proc. 10th Intl. Ship Stability Workshop, Daejeon, Korea.

Belenky, V., C. C. Bassler, and K. Spyrou, 2009, "Dynamic Stability Assessment in Early-Stage Ship Design" Proc. 10th Intl. Conf. on Stability of Ships and Ocean Vehicles, St. Petersburg, Russia.

Bishop, R. C., W. Belknap, C. Turner, B. Simon, and J. H. Kim, 2005, "Parametric Investigation on the Influence of GM, Roll damping, and Above-Water Form on the Roll Response of Model 5613." NSWCCD-50-TR-2005/027.

Levadou, M. and R. Veer, 2006, "Parametric Roll and Ship Design," Proc. 9th Intl. Conf. on Stability of Ships and Ocean Vehicles, Rio de Janeiro, Brazil.

Lin. W. M. and D. K. P. Yue, 1990, "Numerical Solutions for Large Amplitude Ship Motions in the Time-Domain," Proc. of 18th Symp. of Naval Hydrodynamics, Ann Arbor, MI.

Lin. W. M. and D. K. P. Yue, 1993, "Time-Domain Analysis for Floating Bodies in Mild Slope Waves of Large Amplitude," Proc. of 8th Intl Workshop on Water Waves and Floating Bodies, Newfoundland, Canada.

Paulling, J. R., 1961, "The Transverse Stability of a Ship in a Longitudinal Seaway," J. Ship Research, Vol. 4, No. 4, pp. 37-49.

Hashimoto, H., 2009, "Pure Loss of Stability of a Tumblehome Hull in Following Seas," Proc. of the 19th Intl. Offshore and Polar Engineering Conf., Osaka, Japan.

Sarchin, T. H. and L. L. Goldberg, 1962, "Stability and Buoyancy Criteria for US Naval Surface Ships," Trans. SNAME, Vo. 70.

Todd, F. H., 1953, "Some Further Experiments on Single-Screw Merchant Ship Forms," Trans. SNAME, Vol. 61 pp. 516-589.